An EPR characterisation of stable and transient reactive oxygen species formed under radiative and non-radiative conditions

E. Richards, D. M Murphy, M. Che

▶ **To cite this version:**

E. Richards, D. M Murphy, M. Che. An EPR characterisation of stable and transient reactive oxygen species formed under radiative and non-radiative conditions. Research on Chemical Intermediates, 2019, 45 (12), pp.5763-5779. 10.1007/s11164-019-04001-0 . hal-02355558

HAL Id: hal-02355558

https://hal.sorbonne-universite.fr/hal-02355558v1

Submitted on 8 Nov 2019

HAL is a multi-disciplinary open access archive for the deposit and dissemination of scientific research documents, whether they are published or not. The documents may come from teaching and research institutions in France or abroad, or from public or private research centers.

L'archive ouverte pluridisciplinaire **HAL**, est destinée au dépôt et à la diffusion de documents scientifiques de niveau recherche, publiés ou non, émanant des établissements d'enseignement et de recherche français ou étrangers, des laboratoires publics ou privés.

Research on Chemical Intermediates
https://doi.org/10.1007/s11164-019-04001-0

An EPR characterisation of stable and transient reactive oxygen species formed under radiative and non-radiative conditions

E. Richards[1] · **D. M. Murphy**[1] · **M. Che**[2]

Received: 26 August 2019 / Accepted: 6 September 2019
© The Author(s) 2019

Abstract
Electron paramagnetic resonance (EPR) spectroscopy is the ideal method of choice when detecting and studying the wide variety of paramagnetic oxygen-centred radicals. For simple diatomic radicals, such as the superoxide (O_2^-) or peroxy ($ROO^\bullet$) species, the CW EPR profile (in particular the *g*-values) of these species can appear similar and indeed indistinguishable in some cases. Experiments using ^{17}O-enriched oxygen, revealing a rich ^{17}O hyperfine pattern, are therefore essential to distinguish between the two species. However, in many cases, particularly involving TiO_2 photocatalysis, the peroxy-type ($ROO^\bullet$) radicals or other intermediate species such as the [O_2^-…organic]-type adducts can be transient in nature and once again can produce similar *g*-values. In general terms, these reactive oxygen species (ROS) are formed and detected at low-temperature conditions. Hence, the application of EPR spectroscopy to studies of surface-stabilised oxygen-centred radicals must be performed under carefully selected conditions in order to confidently distinguish between the differing types of diatomic radicals, such as O_2^-, $ROO^\bullet$ or [O_2^-…organic].

Keywords EPR spectroscopy · Reactive oxygen species (ROS) · Metal oxides · Isotope exchange · Photocatalysis · Superoxide

This manuscript is dedicated to, and in memory of, the late Prof Michel Che.

✉ D. M. Murphy
MurphyDM@cardiff.ac.uk

[1] School of Chemistry, Cardiff University, Main Building, Park Place, Cardiff CF10 3AT, UK

[2] Laboratoire de Réactivité de Surface, Institut Universitaire de France, Université Pierre et Marie Curie, Paris 6, France

Published online: 21 October 2019

Introduction

The photocatalytic activity of semiconductor metal oxides, such as titanium dioxide (TiO_2), is of considerable interest because of their potential use in a wide range of applications such as water purification [1], solar energy conversion [2] and pollution control [3]. Upon absorption of a photon with energy equal to or greater than the band gap of the semiconductor, an electron/hole pair is generated in the bulk. These charge carriers migrate towards the catalyst surface where they can participate in redox reactions with adsorbed substrate molecules [4–7]. Whilst the bulk oxide properties, such as the optical band gap, are clearly related to catalytic activity, the surface properties are equally important as the reactions obviously occur at this interface. The successful application of metal oxides in photocatalytic reactions relies on very efficient electron-/hole-mediated transfer processes across the surface interface. An understanding of the interfacial chemistry at the molecular level, particularly the nature of surface intermediates which typically involve the formation of reactive oxygen species (ROS), is therefore considered central to the design of more improved photocatalysts.

The nature of the surface oxygen species formed on metal oxides is often dependent on surface morphology, and a vast majority of work in this field has been reported on well-defined single crystal surfaces, using steady-state surface science techniques [8]. However, surface intermediates can also be transient (i.e. thermally unstable) in character and can therefore be difficult to detect and identify using standard spectroscopic techniques. For paramagnetic oxygen species, electron paramagnetic resonance (EPR) spectroscopy is a vital tool in the characterisation of these oxygen-centred radicals and their subsequent reactivity over polycrystalline oxide surfaces. Several research groups have demonstrated how the superoxide radical anion can act as a probe of surface morphology, not only on TiO_2 but also on other polycrystalline metal oxides [9–18]. Although the *g*-values are invaluable in providing important information about the radicals, particularly the surface speciation, the ^{17}O hyperfine tensor is far more informative for determining the electronic structure. The use of oxygen isotopically enriched in ^{17}O ($I = 5/2$) has been particularly valuable in identifying mononuclear [19] and molecular [20] surface oxygen species.

This detailed approach to characterising the radicals is essential when formulating a comprehensive description of the reactive oxygen species involved in surface reactions. For example, superoxide (O_2^-) and organoperoxy ($ROO^\bullet$) radicals often produce similar *g*-values, easily resulting in a misinterpretation of the spectra and hence a mis-assignment of the radical. However, the ^{17}O hyperfine pattern provides a clear and unambiguous means to distinguish between the two species [20]. On the other hand, many reactive oxygen species may be thermally unstable and therefore may not be readily detected in the EPR experiments. In such cases, low-temperature in situ methods are essential to fully inform the experimentalist in studying the surface reaction. In this manuscript, we will demonstrate these two key points by illustrating not only how EPR is used to discriminate between different O_2^- species on oxide surfaces, but also how a class of paramagnetic ROS

involved in oxidation reactions are only visible within a narrow low-temperature range (≈ 140–220 K) and therefore exemplify the need to perform the experiments and measurements under these low-temperature conditions.

Experimental

Materials

O_2^- *on* MoO_3/SiO_2: The samples of supported molybdenum were prepared by a grafting method [21], where $MoCl_5$ was reacted with surface silanol groups in organic media according to the process:

$$MoCl_5 + n\text{SiOH} \rightarrow (\text{SiO})_n MoCl_{5-n} + n\text{HCl}$$

After hydrolysis of the remaining chlorides, the catalyst was washed and dried in air at 120 °C. After transfer into quartz EPR tubes (4 mm thin wall, Wilmad-LabGlass), the samples were first preheated in oxygen at 600 °C then reduced at 600 °C under 100 Torr H_2 for 30 min and finally evacuated to 1×10^{-5} Torr. Oxygen was adsorbed at 77 K at pressures of 10^{-2} to 10^{-1} using $^{16}O_2$ or isotopically enriched $^{17}O_2$ (63 atom % ^{17}O, Icon Isotopes) to produce the O_2^- superoxide ions.

O_2^- *on Polypropylene*: Powdered isotactic polypropylene was obtained from lCl Ltd. The samples were evacuated for 48 h at 100 °C and 1×10^{-5} Torr and then γ-irradiated in vacuo at room temperature with a ^{60}Co source to a dose of 70 Mrad. The gaseous radiation products were evacuated and the samples transferred under vacuum in EPR tubes. Oxygen was added under 3 Torr to form the corresponding peroxy radicals. The labelled peroxy radicals were obtained by adsorption of ^{17}O-enriched oxygen.

ROS on TiO_2: The polycrystalline TiO_2 (Degussa P25) was placed in an EPR cell and heated to 423 K under dynamic vacuum (10^{-4} Torr) overnight to remove any physisorbed water from the surface. The temperature was subsequently raised over 5 h to a final temperature of 773 K and left at this temperature for 1 h. This produced a non-stoichiometric, blue-coloured sample due to the excess of Ti^{3+} centres. The reduced sample was cooled prior to exposure to molecular oxygen and selected organic substrates. The organic substrates (including methanol, toluene and acetonitrile) were exposed to the sample at 77 K, followed by annealing to a series of elevated temperatures (200–260 K) for a period of 10 min. In some experiments, co-adsorbed mixtures of oxygen and the organic substrate were premixed in the vacuum manifold (with a ratio of 1:10) prior to exposure to the TiO_2 surface at 298 K. All UV irradiations were performed at 77 K using a broadband (250–2500 nm) 1000-W UV lamp (Oriel Instruments, 66021), incorporating a water filter for removal of infrared frequencies.

EPR spectroscopy: The EPR spectra were obtained using a continuous wave (CW) Varian (E3 or CS – E109) or Bruker EMX spectrometer operating at ca. 9.3 GHz (X-band), with 100 kHz field modulation and optimised field modulation depth for maximum resolution of spectral features. All measurements were

performed at low temperatures ($T = 77$ or 140 K) or room temperature (as reported in the figure captions).

Results and discussion

EPR characterisation of superoxide species on MoO_3/SiO_2

The superoxide radical can be easily formed by the exposure of a H_2-reduced MoO_3/SiO_2 sample to molecular oxygen. After the reducing treatment in hydrogen, the grafted molybdenum sample exhibited a composite EPR spectrum due to Mo^{5+} ions, as detailed in the earlier work [22]. The adsorption of $^{16}O_2$ at 77 K onto this reduced sample led to a large decrease in the Mo^{5+} signal and the corresponding appearance of a rhombic EPR signal characterised by the g-values of $g_{zz} = 2.017$, $g_{yy} = 2.009$ and $g_{xx} = 2.002$. The reduction in the Mo^{5+} signal intensity and the appearance of the new EPR signal can be attributed to an electron transfer event from the reduced oxide surface to the adsorbed molecular oxygen, forming a surface-stabilised superoxide ion O_2^- on Mo^{6+} [23, 24]. When similar experiments were repeated using ^{17}O-enriched oxygen, the new EPR spectrum (Fig. 1) was produced which revealed a complex hyperfine structure that is far better resolved compared to previous reports for this system [23, 24]. The multiplet patterns arise from the hyperfine coupling of the superoxide ion with the $I = 5/2$ spin of the ^{17}O nucleus. Remarkably, a similar EPR spectrum could also be obtained if a sample containing stabilised $^{16}O_2^-$ ions was subsequently exposed to ^{17}O-enriched oxygen. This result indicates that an

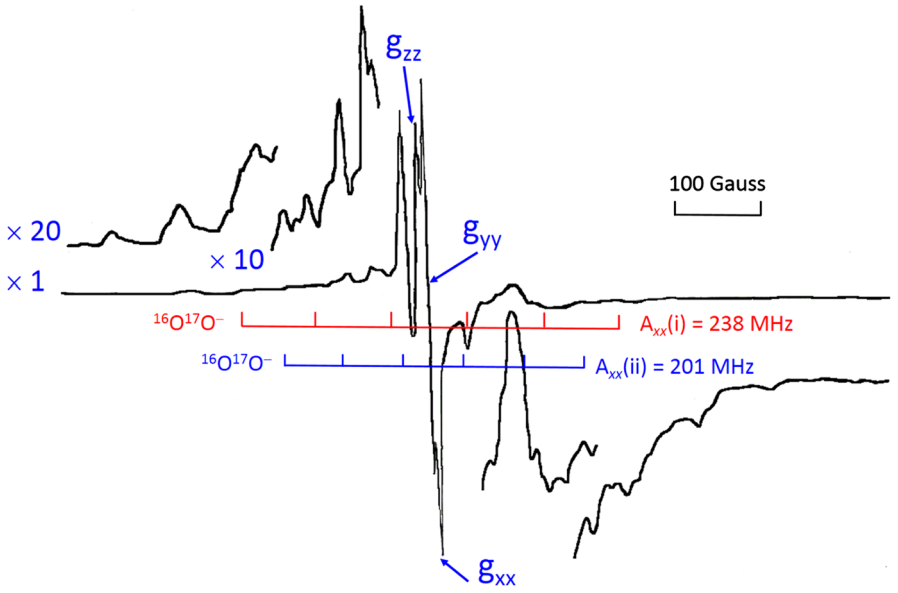

Fig. 1 X-band CW EPR spectrum of $^{17}O_2^-$ on MoO_3/SiO_2 recorded at 77 K, showing the hyperfine interaction with two non-equivalent oxygen nuclei

isotope exchange reaction takes place over the metal oxide surface, as described by Eqs. 1–2 as follows:

$$^{16}O_2^- + {}^{17}O_2 \rightleftharpoons {}^{17}O_2^- + {}^{16}O_2 \quad (1)$$

$$^{16}O_2^- + {}^{16}O^{17}O \rightleftharpoons {}^{16}O^{17}O^- + {}^{16}O_2 \quad (2)$$

In previous reports of superoxide radicals stabilised on TiO_2 or MgO surfaces [20], side-on bonding of the O_2^- ions results in two equivalent oxygen nuclei (i.e. equal spin distribution over both atoms). The resulting EPR spectra in Fig. 1 contain two distinct sets of hyperfine multiplet patterns centred on the lowest g_{xx} component [25, 26]. The first multiplet consists of six hyperfine lines with $A_{xx} = 213$ MHz, indicating the presence of a singly labelled $^{16}O^{17}O^-$ radical. The second multiplet pattern contains 11 hyperfine lines, assigned to a doubly labelled $^{17}O^{17}O^-$ radical. As shown in Fig. 1, the present situation is more complex; indeed, careful analysis indicates that, despite some overlap in the hyperfine lines, two unique sets of six equally spaced lines appear clearly in the spectrum. Both of these sextet multiplet patterns are centred on the same g_{xx} component and are independently characterised by hyperfine coupling values of $A_{xx}(i) = 238$ and $A_{xx}(ii) = 201$ MHz, respectively.

Two explanations may be possible for the observation of these two unique sextet multiplet patterns. The first case labelled (a) in Fig. 2 is that the hyperfine couplings arise from two distinct singly labelled O_2^- anions stabilised on different surface sites, which experience different electrostatic potential interactions with the surface and this results in the distinct hyperfine couplings. In general, O_2^- stabilised at different surface sites should lead to two unique g tensors. In particular, variations are typically observed in the g_{zz} value, due to the sensitivity of this component to the non-degeneracy of the two π_g antibonding orbitals originating from the oxide crystal field [20]. It is also likely that they will respond differently in their rate of formation, reactivity, saturation behaviour or thermal stability, as we have previously demonstrated [26]. It is important to note that this has not been observed in the present case. An alternative description labelled case (b) is based on two slightly inequivalent oxygen nuclei within the same O_2^- radical, which could arise from an end-on binding mode to the oxide surface (Fig. 2).

The choice between the two previous explanations can be made after careful consideration of the outermost hyperfine lines arising from the doubly labelled $^{17}O^{17}O^-$ species. Figure 3 gives a schematic illustration of the multiplet patterns that can

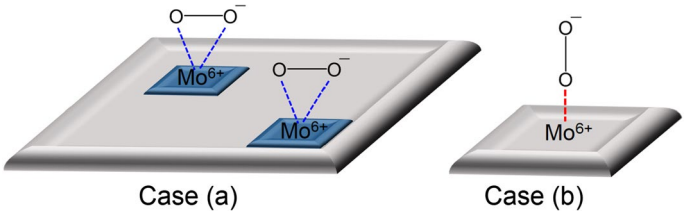

Fig. 2 Schematic illustration of the alternative binding modes of the superoxide O_2^- anion to the MoO_3/SiO_2 surface

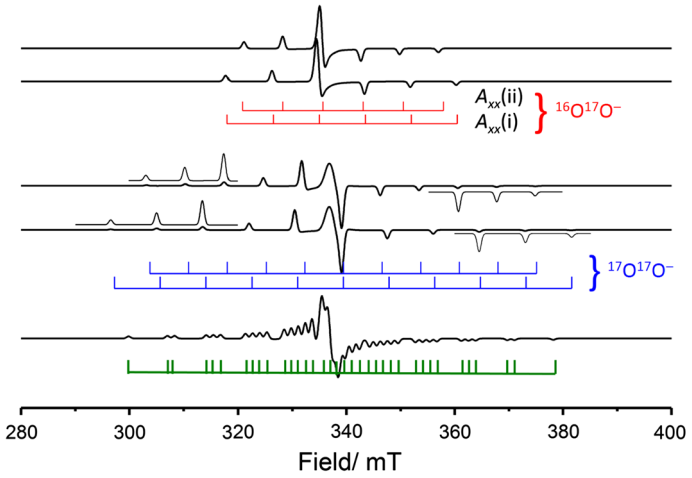

Fig. 3 Computational EPR simulations of the alternative binding modes of the superoxide O_2^- anion on the MoO_3/SiO_2 surface

be expected for the two cases (a) and (b), respectively. It is seen that in case (a), the total number of hyperfine lines amounts to $[(2\times6)+(2\times11)]=34$, with a total spectral width of $[10\times A_{xx}(i)]$ assuming that $A_{xx}(i)>A_{xx}(ii)$, where $A_{xx}(i)$ and $A_{xx}(ii)$ refer to the hyperfine splittings for labelled O_2^- in the two types of sites. For case (b), the total number of hyperfine lines is $[(2\times6)+(6\ x\ 6)]=48$ with a total spectral width of $[5\times(A_{xx}(i)+A_{xx}(ii))]$, with $A_{xx}(i)>A_{xx}(ii)$, assuming that $A_{xx}(i)$ and $A_{xx}(ii)$ refer to the inner and outer oxygen relative to the surface, respectively. In fact, the total number of hyperfine lines observed is expected to be smaller than the calculated maximum because of the overlap between the lines. Analysis of the outermost $^{17}O^{17}O^-$ lines in Fig. 1 shows that the total spectral width is 2211 MHz (=787 Gauss). Taking $A_{xx}(i)=238$ MHz and $A_{xx}(ii)=201$ MHz, as characterised from the two distinct sextet patterns, the total spectral width clearly closely corresponds with $[5\times(238+201)]=2195$ MHz and not $[10\times201]=2010$ MHz. This result clearly indicates that for O_2^- stabilised on MoO_3/SiO_2, there are two inequivalent oxygen nuclei in the same O_2^- adsorbed at one type of surface site, corresponding to the situation described by case b).

The observation of oxygen isotopic exchange (OIE) over the MoO_3/SiO_2 surface is in agreement with previous reports on other oxides [27–31]. Indeed, the study of OIE is an effective way for understanding the reactivity of oxygen species on oxide surfaces but has previously been observed to involve exchange of surface oxygen atoms with atoms in the gas phase, via Eqs. 3–4 as follows:

$$^{18}O_2(g) + {}^{16}O_s \rightarrow {}^{18}O^{16}O\ (g) + {}^{18}O_s \tag{3}$$

$$^{18}O_2(g) + 2{}^{16}O_s \rightarrow {}^{16}O_2(g) + 2{}^{18}O_s \tag{4}$$

EPR characterisation of superoxide species over γ-irradiated polypropylene

It is well known that γ-irradiation of polymers leads to chain scission events and ultimately an abundance of reactive carbon-based radicals. These radicals can readily react with molecular oxygen (at least for the surface accessible radicals resulting from rapid O_2 diffusion through the polymer). Upon γ-irradiation of isotactic polypropylene, followed by exposure to molecular oxygen, the EPR spectrum shown in Fig. 4 is observed at 77 K. The predominant axial spectrum is characterised by the g-values of $g_{zz} = 2.0351$, $g_{yy} = 2.0081$ and $g_{xx} = 2.0024$, and this signal can be readily assigned to stabilised peroxy radicals ($ROO^{\bullet}$), in agreement with previous reports [32–35].

When the same experiment is performed in the presence of ^{17}O-enriched oxygen, a more complex EPR spectrum is obtained with a rich hyperfine multiplet pattern (Fig. 5). Detailed analysis of the hyperfine coupling centred on the g_{xx} component resolves two unique multiplets, characterised by $A_{xx}(I) = 276$ MHz (98.5 Gauss) and $A_{xx}(II) = 168$ MHz (60 Gauss). The substantial difference between the magnitudes of the two hyperfine couplings is indicative of two inequivalent oxygen atoms, indicating an end-on interaction of the molecular oxygen with the carbon-based $R^{\bullet}$ radicals generated in the polymer during γ-irradiation. The hyperfine couplings, $A_{xx}(I)$ and $A_{xx}(II)$, are therefore assigned to the inner and outer oxygens atoms, respectively, within this diatomic $ROO^{\bullet}$ centre. Notably, when the sample containing surface-stabilised peroxy radicals is annealed between 77 and 298 K, no change in the EPR spectrum is detected. This observation indicates the thermal stability of the peroxy radicals in the polymer material, where extensive mobility of the radical is not permitted unlike the

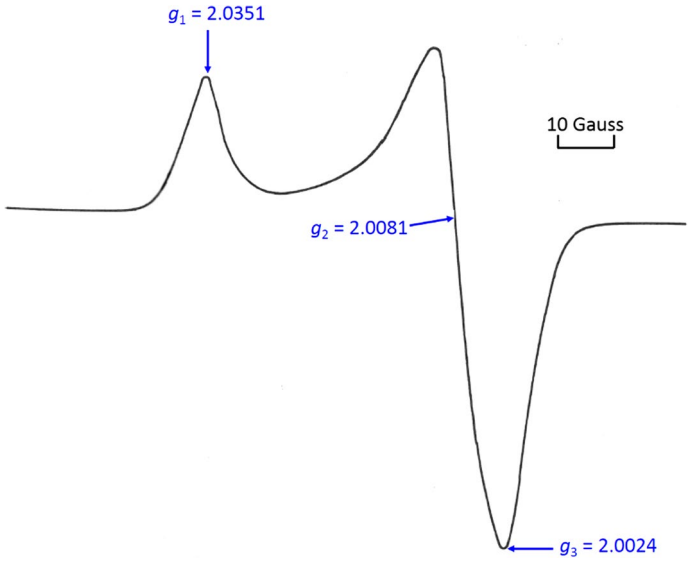

Fig. 4 CW X-band EPR spectra (77 K) of O_2^- formed by O_2 exposure to γ-irradiated polypropylene

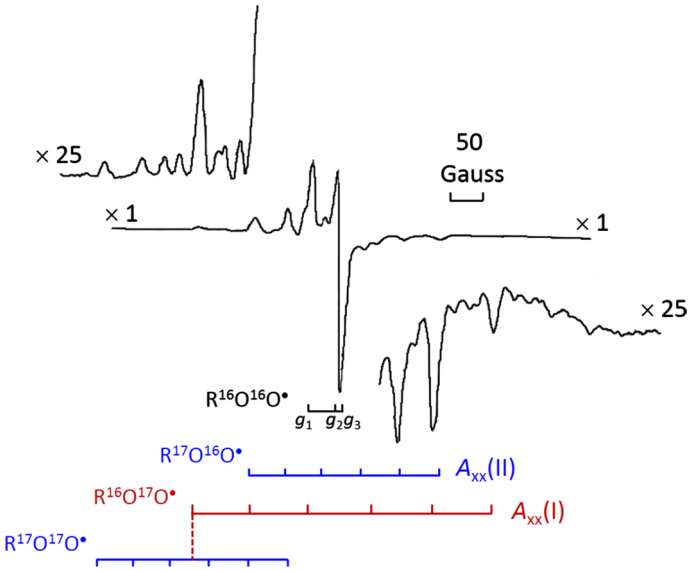

Fig. 5 CW X-band EPR spectra (77 K) of $^{17}O_2^-$ formed by $^{17}O_2$ exposure to γ-irradiated polypropylene

situation observed on metal oxide surfaces where the radicals are only weakly adsorbed.

EPR characterisation of superoxide reactivity and ROS on TiO_2

In the previous section, describing the EPR characterisation of the O_2^- centres, the radical in question on the MoO_3/SiO_2 surface was thermally stable. This is a frequently observed case for O_2^- on several other oxide surfaces including TiO_2, regardless of the original method used to generate the radical [9, 20, 36, 37]. However, surface intermediates, in particular reactive oxygen species (ROS), can also be transient (i.e. thermally unstable) in nature and can therefore be difficult to directly detect and study. In many cases, it is well known that oxygen-based radicals (including O_2^-) on TiO_2 are essential to many photooxidation processes [38–40]. Indeed, EPR has often been used to monitor the reactivity of the oxygen-centred radicals in various oxidation-based surface reactions [20]. In previous work, we have demonstrated how a series of transient organoperoxy radicals ($ROO^\bullet$) can play a contributory role in the decomposition of acetone and acetonitrile over TiO_2 [41, 42], but these species are only stable and therefore visible at temperatures lower than 200 K (unlike O_2^- which is readily detected at room temperature). Therefore, in this section, we will evidence how organic substrates react with superoxide radicals over polycrystalline TiO_2 surfaces under dark conditions leading to transient ROS.

Similar to the case reported for acetone [41], a thermally unstable ROS was observed when acetonitrile (CH_3CN) was exposed to a TiO_2 sample that contained preformed O_2^- radicals (i.e. O_2^-/TiO_2); the O_2^- centres were readily formed by

exposure of molecular oxygen to thermally reduced TiO_2 [42]. The ROS was identified as a transient [O_2^-…CH_3CN] adduct, characterised by the g-values listed in Table 1. An analogous surface species was also observed with acetone, i.e. [O_2^-…CH_3COCH_3] [41]. These species are thermally unstable and decompose at temperatures $T > 220$ K. During the reaction between surface O_2^- and acetonitrile, a second radical is also formed and identified as the hydroperoxy ($HO_2^\bullet$) species, with spin Hamiltonian parameters of $g_1 = 2.028$, $g_2 = 2.010$, $g_3 = 2.004$, $^{H}A_1 = 34.1$ MHz (1.2 mT), $^{H}A_2 = 28.1$ MHz (1.0 mT) and $^{H}A_3 = 28.0$ MHz (1.0 mT) [42]. We therefore wanted to explore whether these transient surface adducts, abbreviated hereafter using the generic label [O_2^-…organic], are common to other organic substrates, such as methanol and toluene.

To probe whether a transient [O_2^-…CH_3OH] surface adduct could be formed, analogous to the [O_2^-…CH_3CN] [42] and [O_2^-…CH_3COCH_3] [41] adducts, methanol (10 Torr) was exposed to a O_2^-/TiO_2 sample. Room temperature exposure of the methanol vapours to this sample resulted in the immediate disappearance of the O_2^- EPR signals. However, when the methanol was admitted to O_2^-/TiO_2 at 77 K, followed by thermal annealing between T = 200 K and 240 K, a gradual decrease in the O_2^- signal intensity was observed. Simultaneously, a new peak emerged in the g_{zz} region with $g \sim 2.028$ (Fig. 6), due to the formation of a new radical centre.

As described previously by us [26, 43], the site-specific O_2^- centres on TiO_2 (labelled sites I, II and III in Fig. 6) slowly decay due to reaction of O_2^- with the organic substrate (methanol in this case), accompanied by the appearance of the new signal at $g \sim 2.028$. This latter signal grows in intensity as the temperature is increased, before decaying at $T > 220$ K. The reactivity between CH_3OH and O_2^- appears to be non-site selective, analogous to the situation observed with acetonitrile where all three O_2^- sites I, II and III react readily with the substrate. The peaks labelled * in Fig. 6 are assigned to the $HO_2^\bullet$ species, possessing similar g- and ^{H}A-values to those given above for acetonitrile. This assignment to $HO_2^\bullet$ was confirmed in the current case using fully deuterated methanol (CD_3OD); in this latter case, the superhyperfine peaks arising from the $^2HO_2^\bullet$ were not visible in the EPR spectrum, as expected due to the smaller magnetic moment of ^2H compared to ^1H.

The above experiment with methanol was also repeated using toluene, and the resulting EPR spectra are shown in Fig. 7. Addition of toluene to O_2^-/TiO_2 at room

Table 1 Spin Hamiltonian parameters for the family of reactive oxygen species (ROS) formed over TiO_2, including [O_2^-…organic] and ROO$^\bullet$

Substrate	Species	g_1	g_2	g_3
Acetonitrile	[O_2^-…CH_3CN]	2.031	2.01	2.003
	$NCCH_2OO^\bullet$	2.034	2.007	2.002
Methanol	[O_2^-…CH_3OH]	2.027	2.01	2.003
	$HOCH_2OO$	2.034	2.007	2.002
Toluene	[O_2^-…$C_6H_5CH_3$]	2.025	2.01	2.004
	$C_7H_7OO^\bullet$	2.034	2.001	2.004
Acetone	[O_2^-…CH_3COCH_3]	2.035	2.008	2.003
	$CH_3COCH_2OO^\bullet$	2.034	2.007	2.001

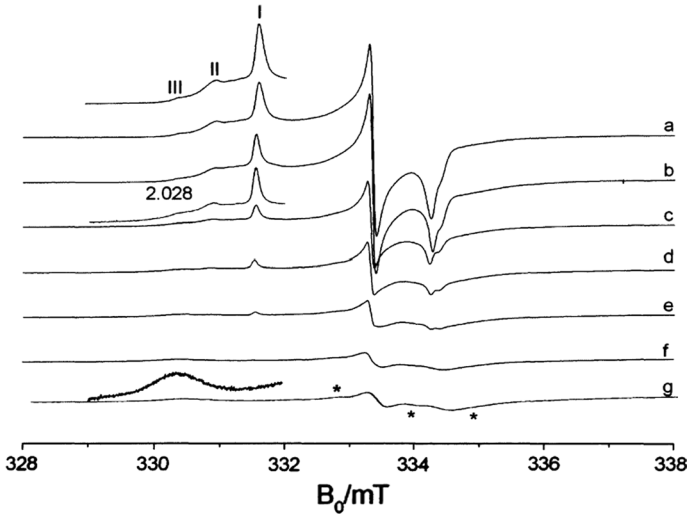

Fig. 6 CW X-band EPR spectra (130 K) of (a) O_2^- formed on a thermally reduced TiO_2 sample (reduced at 773 K) and after exposure of this O_2^-/TiO_2 sample to methanol (10 Torr) at 77 K followed by annealing to (b) 140, (c) 210, (d) 215, (e) 220, (f) 225 and (g) 230 K

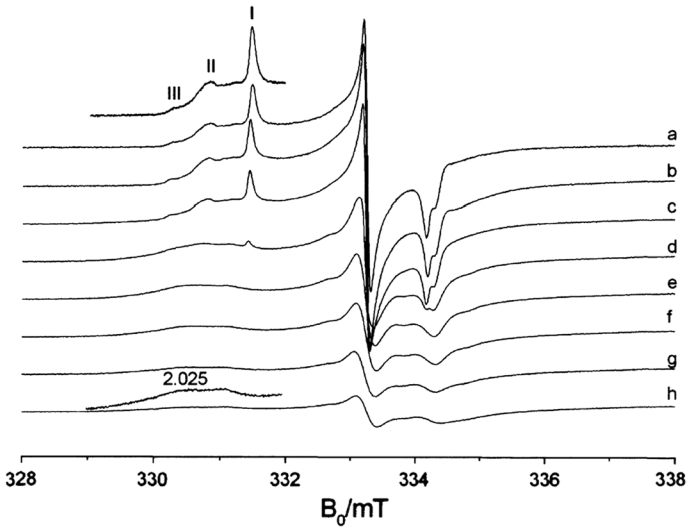

Fig. 7 CW X-band EPR spectra (130 K) of (a) O_2^- formed on a thermally reduced TiO_2 sample (reduced at 773 K) and after exposure of this sample to toluene (10 Torr) at 77 K followed by annealing to (b) 140, (c) 215, (d) 230, (e) 240, (f) 245, (g) 255 and (h) 265 K

temperature resulted in the complete loss of the superoxide signals, as the toluene reacts with and destroys the O_2^- centres. However, upon addition of toluene at 77 K, followed by gradual annealing to elevated temperatures (200–265 K), a gradual decrease in the O_2^- signal intensity accompanied by the gradual appearance of a

new peak in the g_{zz} region at $g \sim 2.025$ was observed (Fig. 7). Unlike the previous methanol case, the reactivity of toluene with O_2^- now appears to be site specific. As evident from Fig. 7, the O_2^- site I species (previously assigned to a superoxide centre stabilised in close proximity to a surface vacancy site, labelled [Vac…O_2^-] [41]) reacts preferentially with toluene relative to O_2^- sites II–III (the non-vacancy stabilised O_2^- centres) [41]. The reason why [Vac…O_2^-] would react differently compared to the non-vacancy stabilised O_2^- centres with toluene compared to methanol is not currently understood, but clearly these results show the interesting variable behaviour of heterogeneous site-specific O_2^- reactivity on TiO_2. The $HO_2^{\bullet}$ species is also formed when toluene reacts with O_2^-/TiO_2, and once again this assignment was confirmed using fully deuterated toluene resulting in the loss of ^{H}A signals from the EPR spectrum (Fig. 7). The signal at $g \sim 2.025$ appears most intense at $T = 265$ K and can be assigned to the transient [O_2^-…$C_6H_5CH_3$] adduct. This species then decays at more elevated temperatures above 265 K.

Owing to the considerable overlap of the g components for both O_2^- and [O_2^-…$C_6H_5CH_3$], the precise assignment of the g_1 and g_2 components for the latter adduct is difficult to extract. As a result, the experiment was repeated using TiO_2 thermally reduced at lower temperatures (623 K). The lower reduction temperature decreases the extent of O_2^- speciation on TiO_2, so that only one O_2^- centre (site I with $g_1 = 2.019$, $g_2 = 2.011$ and $g_3 = 2.005$) predominates, thereby considerably simplifying the spectrum. Toluene was then exposed to the site I dominated O_2^-/TiO_2 sample, and the resulting spectra are shown in Fig. 8. Owing to the improved resolution, the experimental spectrum for [O_2^-…$C_6H_5CH_3$] could be simulated with greater confidence; the extracted spin Hamiltonian parameters are listed in Table 1.

In the above cases for methanol and toluene (and previously reported for acetonitrile [42] and acetone [41]), the organic substrates were exposed to the thermally

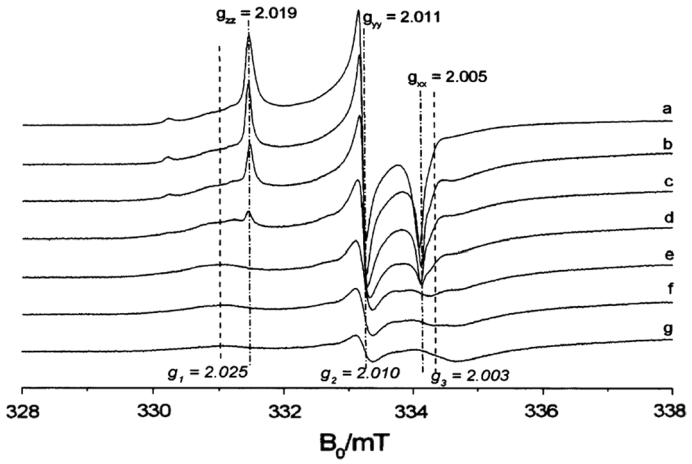

Fig. 8 CW X-band EPR spectra (130 K) of (a) O_2^- formed on a thermally reduced TiO_2 sample (reduced at 623 K) and after exposure of this sample to toluene (10 Torr) at 77 K followed by annealing to (b) 130, (c) 220, (d) 230, (e) 240, (f) 250 and (g) 260 K. The g-values for O_2^- and [O_2^-…$C_6H_5CH_3$] are highlighted with the dash-dot and dash lines, respectively

reduced TiO_2 sample containing the O_2^- centres. However, we were also interested in exploring whether the route to O_2^- formation has any bearing on the subsequent reactivity of O_2^-. In the next series of experiments, the O_2^- centres were therefore generated over TiO_2 using UV irradiation, i.e. to test whether $O^-_{2\,(thermal)}/TiO_2$ behaves and reacts differently with the organic substrates compared to $O^-_{2\,(UV)}/TiO_2$. The results obtained by reacting the O_2^- with acetonitrile are shown in Fig. 9.

The EPR spectrum of the UV-generated O_2^- species on TiO_2 is shown in Fig. 9a. This signal is considerably more complex compared to the $O^-_{2\,(thermal)}/TiO_2$ (see Figs. 6a, 7a, 8a, for example). The photochemically generated superoxide O_2^- centre has the spin Hamiltonian parameters of $g_{xx} \sim 2.004$, $g_{yy} = 2.011$ and at least six observable g_{zz} values of 2.017 (I'), 2.019 (I), 2.020 (II'), 2.023 (II), 2.025 (II'') and 2.026 (III). The extra sites I' and II' (with $g_{zz} = 2.017$ and 2.025) are due to additional stabilisation sites on the TiO_2 surface which are not available on the thermally reduced surface. Additional peaks in the spectrum (marked #) are due to traces of interstitial photo-generated Ti^{3+} centres (Fig. 9). Acetonitrile was subsequently added to this $O^-_{2\,(UV)}/TiO_2$ sample at 77 K. Upon annealing under the acetonitrile atmosphere, the O_2^- signal intensity decreased, and this was accompanied by the appearance of a new signal at $g \sim 2.032$ (Fig. 9b–h). This new signal was first observed at $T \sim 210$ K and begins to decay irreversibly at $T > 250$ K; this signal can once again be assigned to the transient $[O_2^- \ldots CH_3CN]$ adduct.

The main difference between the thermally treated [42] and photoirradiated samples (Fig. 9) is the lower overall intensity of the $[O_2^- \ldots CH_3CN]$ adduct on the photoirradiated sample. The reason for this is simply due to the lower initial abundance of UV-generated O_2^-. Nevertheless, there appears to be no appreciable difference

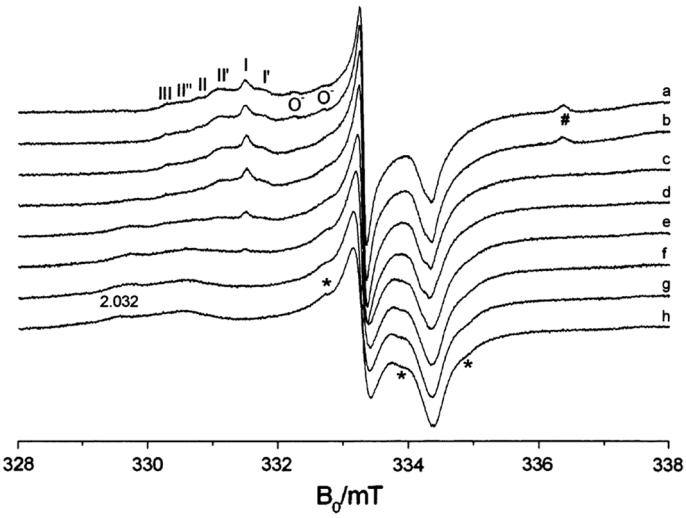

Fig. 9 CW X-band EPR spectra (130 K) of (a) O_2^- formed photochemically by UV irradiation of TiO_2 containing adsorbed molecular O_2. After $O^-_{2\,(UV)}$ formation, the excess O_2 was evacuated prior to exposure of this sample to acetonitrile (7.3 Torr) at 77 K followed by annealing to (b) 140, (c) 190, (d) 200, (e) 210, (f) 215, (g) 220 and (h) 230 K

observed in the reactivity of acetonitrile with $O_{2\,(thermal)}^-/TiO_2$ and $O_{2\,(UV)}^-/TiO_2$. The formation of the radical species $[O_2^-\ldots CH_3CN]$ and $HO_2^\bullet$ is observed in both cases. This is an important result as it shows that these transient $[O_2^-\ldots CH_3CN]$ adducts can be formed from O_2^- radicals generated under both thermal and photochemical conditions.

As previously evidenced by us using ^{17}O-labelled oxygen [26], the O_2^- centres in the adducts have equivalent oxygen atoms, unlike the inequivalent spin densities that would be expected in the peroxy case [42]. This indicates a side-on manner of interaction between O_2^- and the organic substrates. The resulting series of EPR spectra for these transient $[O_2^-\ldots organic]$ adducts with acetone, acetonitrile, methanol and toluene are summarised in Fig. 10. We have previously postulated that the formation of the transient adducts arises from the nucleophilic attack by the O_2^- anion on the electrophilic carbon atom of the organic substrate [41]. If the strength of this interaction is dependent on the electrophilic nature of the carbon to which it is attached, the series of substrates presented in Fig. 10 can provide insights into how this interaction is affected. The relative electron-withdrawing power of the functional groups to which the CH_3 group is attached is C_6H_5 (toluene) < OH (methanol) < CO (acetone) ~ CN (acetonitrile). The g_1 values for the resulting $[O_2^-\ldots organic]$ species then mirror this trend, as indicated in Fig. 10 and Table 1.

In all of the above-cited experiments, the organic substrates (methanol and toluene) were exposed to TiO_2-containing surface-stabilised O_2^- centres. However, previous work from our group revealed how direct UV irradiation of TiO_2 containing co-adsorbed mixtures of O_2/organic substrates can yield a series of transient organoperoxy and peroxyacyl reactive oxygen species in the presence of ketones [41, 43] and aldehydes [44] which are formed via hole-mediated processes (vide infra). To explore this photochemistry in greater detail, a co-mixture of acetonitrile plus O_2

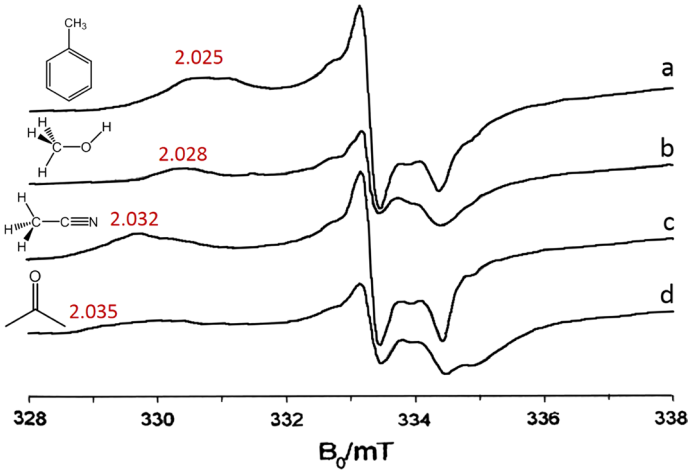

Fig. 10 CW EPR spectra (120 K) of the transient $[O_2^-\ldots organic]$ adducts formed on O_2^-/TiO_2 after addition of (a) toluene, (b) methanol, (c) acetonitrile and (d) acetone. The organic substrates were added at 77 K and the sample subsequently annealed to ~ 220 K

was added to a TiO_2 sample in a ratio of 10:1 (total pressure = 15 Torr) to ensure the organic substrate was in excess. The sample was then cooled to 77 K and exposed to UV radiation at this temperature for 30 min. After annealing the sample to 130 K, the excess gas was removed before recording the EPR spectrum (Fig. 11). Similar experiments were also performed using methanol and toluene with similar results (data not shown here). Confirmation of the assignment to the peroxy radicals with methanol and toluene is currently underway in our laboratory using enriched $^{17}O_2$.

The EPR spectrum of UV-radiated TiO_2 containing acetonitrile–O_2 is dominated by an orthorhombic signal with g-values of $g_1 = 2.034$, $g_2 = 2.010$ and $g_3 = 2.004$; additional signals at $g = 1.989$ and $g \sim 1.972$ (labelled * in Fig. 11) are also formed, which can be easily assigned to bulk Ti^{3+} cations at substitutional and lattice sites (generated during low-temperature irradiation of the TiO_2) [45–47]. The orthorhombic signal is thermally unstable; upon warming to elevated temperatures ($T > 180$ K), the signal intensity progressively decreases (not shown here) until eventually it is completely lost at 298 K. However, this signal can be regenerated by admission of an additional dose of CH_3CN/O_2 followed by re-irradiation of the sample at 77 K. The signal was only observed with a high CH_3CN/O_2 ratio; if molecular oxygen is abundant, a signal corresponding to the photo-generated O_2^- centres is observed.

The spin Hamiltonian parameters for this new signal are somewhat reminiscent of the earlier [O_2^-…CH_3CN] adduct (Table 1), with one notable exception: the g_1 value of 2.034. The overall spectral profile is in fact identical to that of the organoperoxy species formed with acetone and other ketones [41, 42]. These organoperoxy-type intermediates, formed after irradiation of a co-adsorbed mixture of organic–O_2 have been identified over TiO_2 and are typically characterised by the spin Hamiltonian parameters of $g_1 = 2.034$, $g_2 = 2.010$ and $g_3 = 2.003$. These values compare favourably with those observed here (Fig. 11); therefore, taking into consideration the similar thermal behaviour, this new species can be readily assigned to an organoperoxy-type radical

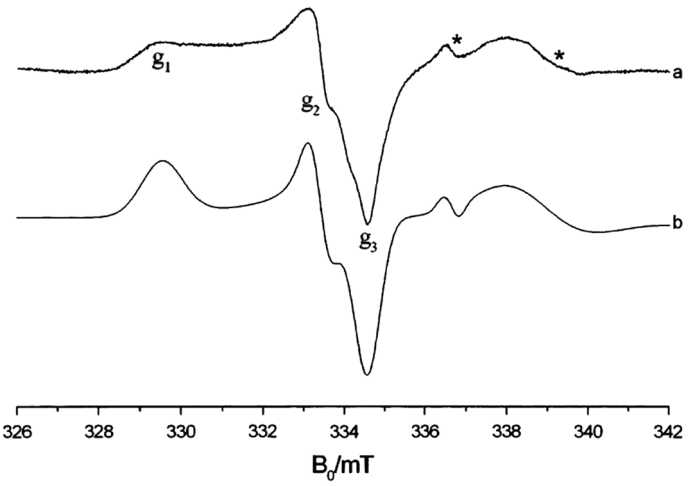

Fig. 11 Experimental (a) and simulated (b) CW X-band EPR spectrum (130 K) of UV-irradiated TiO_2 containing co-adsorbed acetonitrile/O_2 in a 10:1 ratio (total pressure 15 Torr)

$NCCH_2OO^{\bullet}$. Irradiation of TiO_2 results in the generation of an electron (e^-)–hole (h^+) pair. These can either recombine in the bulk or migrate to the surface of TiO_2, where they participate in surface reactions with adsorbed species. The electron can migrate to the surface to form a Ti^{3+} centre, whereas the holes are trapped at surface O^{2-} sites to give O^-. The acetonitrile is adsorbed on the TiO_2 surface at Lewis acid sites and is quickly deprotonated by H^+ transfer to produce a hydroxyl group and $NCCH_2^{\bullet}$:

$$CH_3CN + O^- \rightarrow NCCH_2^{\bullet} + OH^- \quad (5)$$

The resulting radical cation can then react with molecular oxygen forming the peroxy radical:

$$CNCH_2^{\bullet} + O_2 \rightarrow NCCH_2OO^{\bullet} \quad (6)$$

A similar mechanism for the formation of these organoperoxy ($ROO^{\bullet}$)-type radicals has been identified in the literature for the photooxidation of ketones [41] and ethylene [48] on TiO_2; in the latter case, the g-values were $g_1 = 2.034$, $g_2 = 2.010$ and $g_3 = 2.001$. In the present work, similar EPR spectra were also obtained using methanol and toluene (Table 1).

It is therefore clear that a series of transient organoperoxy radicals ($ROO^{\bullet}$) can be formed after UV irradiation of an organic–O_2 mixture (organic substrate = acetonitrile, acetone, methanol and toluene) over TiO_2. These radicals are formed by hole-mediated processes, generating organic radical anions which rapidly react with molecular oxygen to form the resulting organoperoxy centres. The transient species all decay above $T > 190$ K, but can be easily regenerated and all produce analogous g-values. Unlike the aforementioned [O_2^-…organic] centres with characteristic and independent g_1 values (Table 1), the g_1 value of 2.034 is constant and independent of the organic substrate used. Sevilla et al. [49] showed that different organic substituents (R) have little effect on the reactivity and structure of $ROO^{\bullet}$ peroxy radicals with the g-values for carbon-based peroxy radicals varying only slightly for different substituents. The nature of the R substituent, however, can affect the stability of the radical, and this may explain the different signal intensities which we observed for these radicals using the different organic substrates, i.e. the signals were weaker for methanol and toluene.

The thermal instability of these $ROO^{\bullet}$ intermediates highlights the necessity to experimentally undertake in situ (EPR spectroscopy) measurements as other spectroscopic techniques may be unable to provide this low-temperature identification. The identification of these peroxy intermediates is also important as it shows how different surface treatments can result in the formation of different species. The organoperoxy radicals have been identified with aldehydes [44], ketones [41, 43], acetonitrile [42] and in this work with alcohols and toluene, indicating that this type of intermediate plays a key role in photooxidation processes using a variety of substrates.

Conclusions

The superoxide radical anion (O_2^-) is readily formed over MoO_3/SiO_2 by the exposure of the reduced sample to molecular oxygen, as widely reported. However, whilst the CW EPR spectrum of the unlabelled species is consistent with a surface

$^{16}O_2^-$ centre, analysis of the spectrum obtained using ^{17}O-enriched oxygen is necessary to fully interpret the nature of the radical which reveals the presence of an end-on bonded O_2^- species. The same $^{17}O_2^-$ species could be formed from $^{16}O_2^-$ by the exposure of the sample to ^{17}O-enriched molecular oxygen in an isotope exchange reaction. In principle, whilst side-on and end-on bonded O_2^- species can exist on MoO_3/SiO_2, the latter species appear to dominate.

Paramagnetic oxygen-based radicals are also readily formed when molecular oxygen is exposed to γ-irradiated polypropylene. In this case, the CW EPR signal has notably broad linewidths. The profile of the spectrum is analogous to that expected of a generic ROS entity, with $g_1 = 2.035$, $g_2 = 2.008$ and $g_3 = 2.002$, but once again only a definitive assignment to an end-on peroxy radical ($ROO^\bullet$) can be made using ^{17}O hyperfine pattern.

A number of oxygen-centred radicals have been proposed to play a key role in the degradation of organic substrates over TiO_2 under dark conditions or under UV irradiation. Here, we have shown how the decomposition of acetonitrile, methanol and toluene can occur over O_2^-/TiO_2. The reaction of the organic substrates with O_2^- results in the production of a transient and thermally unstable (above 240 K) surface adduct, labelled [O_2^-…organic]. These adducts are characterised by the EPR g-values of $g_1 = 2.031$-2.025, $g_2 = 2.010$ and $g_3 = 2.003$, and similar to previously published data appear to possess a side-on arrangement of the organic molecule with respect to the two equivalent oxygen atoms of O_2^-. Additionally, a hydroperoxy ($HO_2^\bullet$) radical was also formed under these experimental conditions. This [O_2^-… organic] adduct can be formed regardless of how the O_2^- radical was originally generated.

Furthermore, a series of thermally unstable surface-organoperoxy-type radical intermediates were also identified following UV irradiation of a series of co-adsorbed organic–O_2 mixtures. These transient radicals ($NCCH_2OO^\bullet$, $HOCH_2OO^\bullet$, $C_7H_7OO^\bullet$) produced after UV irradiation all possessed analogous g-values ($g_1 = 2.034$, $g_2 = 2.007$, $g_3 = 2.001$). The signal intensities for the $HOCH_2OO^\bullet$ and $C_7H_7OO^\bullet$ radicals were much weaker compared to those of the $NCCH_2OO^\bullet$ species (possibly due to the different stabilities of the respective radicals and the different competing reactions that can occur with these substrates over the TiO_2 surface).

The work presented in this paper demonstrates the complexity of organic substrate decomposition with ROS over TiO_2. It is clear that these substrates can react and degrade under dark conditions (non-radiative) via a reaction with surface O_2^- radicals forming transient [O_2^-…organic] adducts, or via UV irradiation conditions where hole-mediated processes lead to the formation of $ROO^\bullet$ species. In all cases, the nature of the transient reactive oxygen species (ROS) in TiO_2 photocatalysis is very important and highlights the need to perform low-temperature in situ measurements to obtain a complete picture on the oxidation radical steps.

Open Access This article is distributed under the terms of the Creative Commons Attribution 4.0 International License (http://creativecommons.org/licenses/by/4.0/), which permits unrestricted use, distribution, and reproduction in any medium, provided you give appropriate credit to the original author(s) and the source, provide a link to the Creative Commons license, and indicate if changes were made.

References

1. Y. Yang, J. Shin, J.T. Jasper, M.R. Hoffmann, Environ. Sci. Tech. **50**, 8780 (2016)
2. B. O'Regan, M. Graetzel, Nature **353**, 737 (1991)
3. J. Schneider, M. Matsuoka, M. Takeuchi, J. Zhang, Y. Horiuchi, M. Anpo, D.W. Bahnemann, Chem. Rev. **114**, 19 (2014)
4. T.L. Thompson, J.T. Yates, Chem. Rev. **106**, 4428 (2006)
5. A. Kudo, Y. Miseki, Chem. Soc. Rev. **38**, 253 (2009)
6. K. Honda, A. Fujishima, Nature **238**, 37 (1972)
7. R.F. Howe, M. Gratzel, J. Phys. Chem. **91**, 3906 (1987)
8. U. Diebold, Surf. Sci. Rep. **48**, 53 (2003)
9. M. Chiesa, E. Giamello, M. Che, Chem. Rev. **110**, 1320 (2010)
10. J.M. Coronado, J. Soria, Catal. Today **123**, 37 (2007)
11. C. Murata, T. Hattori, H. Yoshida, J. Catal. **231**, 292 (2005)
12. E. Giamello, E. Garrone, P. Ugliengo, J. Chem. Soc. Faraday Trans. **85**, 1373 (1989)
13. E. Giamello, E. Garrone, P. Ugliengo, A.J. Che, J. Tench, J. Chem. Soc. Faraday Trans. **85**, 3987 (1989)
14. M. Chiesa, M.C. Paganini, E. Giamello, C. Di Valentin, G. Pacchioni, Acc. Chem. Res. **39**, 861 (2006)
15. M. Chiesa, M.C. Paganini, G. Spoto, E. Giamello, C. Di Valentin, A. Del Vitto, G. Pacchioni, J. Phys. Chem. B **109**, 7314 (2005)
16. M. Chiesa, M.C. Paganini, E. Giamello, D.M. Murphy, J. Phys. Chem. B **105**, 10457 (2001)
17. M. Anpo, M. Che, B. Fubini, E. Garrone, E. Giamello, M.C. Paganini, Top. Catal. **8**, 189 (1999)
18. K. Sobanska, A. Krasowska, T. Mazur, K. Podolska-Serafin, P. Pietrzyk, Z. Sojka, Top. Catal. **58**, 796 (2015)
19. M. Che, A.L. Tench, Adv. Catal. **31**, 77 (1982)
20. M. Che, A.L. Tench, Adv. Catal. **32**, 1 (1983)
21. C. Louis, M. Che, F. Boson-Verduras, J. Chem. Phys. **79**, 000 (1982)
22. M. Dufaux, M. Che, C. Naccache, Compt Rend. de Seanc. de l'Academie des Sci. C **268**, 2255 (1969)
23. Y.B. Taarit, J.H. Lunsford, J. Phys. Chem. **77**, 780 (1973)
24. M. Shiotani, G. Moro, J.H. Freed, J. Chem. Phys **74**, 2616 (1981)
25. A.J. Tench, P. Holroyd, Chem. Commun. **8**, 471 (1968)
26. E. Carter, A.F. Carley, D.M. Murphy, J. Phys. Chem. C **111**, 10630 (2007)
27. R.V. Mikhaylov, A.A. Lisachenko, V.V. Titov, J. Phys. Chem. C **116**, 23332 (2012)
28. R.V. Mikhaylov, N.I. Glazkova, K.V. Nikitin, J. Photochem. Photobiol. A **332**, 554 (2017)
29. H. Courbon, M. Formenti, P. Pichat, J. Phys. Chem. **81**, 550 (1977)
30. X. Pang, C. Chen, H. Ji, Y. Che, W. Ma, J. Zhao, Molecules **19**, 16291 (2014)
31. S. Sato, J. Phys. Chem. **91**, 2895 (1987)
32. D. Olivier, C. Marachi, M. Che, J. Chem. Phys. **72**, 3348 (1980)
33. D. Olivier, C. Marachi, M. Che, J. Chem. Phys. **71**, 4688 (1979)
34. M. Che, A.J. Tench, J. Chem. Phys. **64**, 2370 (1976)
35. M. Che, A.J. Tench, J. Polym. Sci. C Polym. Lett. **13**, 345 (1975)
36. M. Chiesa, E. Giamello, M.C. Paganini, Z. Sojka, D.M. Murphy, J. Chem. Phys. **116**, 4266 (2002)
37. A.L. Attwood, D.M. Murphy, J.L. Edwards, T.A. Egerton, R.W. Harrison, Res. Chem. Intermed. **29**, 449 (2003)
38. S.B. Kim, H.T. Hwang, S.C. Hong, Chemosphere **48**, 437 (2002)
39. R. Nakamura, S. Sato, J. Phys. Chem. B **106**, 5893 (2002)
40. M.A. Henderson, C.L. Perkins, C.H.F. Peden, U. Diebold, J. Phys. Chem. B **103**, 5328 (1999)
41. E. Carter, A.F. Carley, D.M. Murphy, ChemPhysChem **8**, 113 (2007)
42. J. Green, E. Carter, D.M. Murphy, Res. Chem. Intermed. **35**, 145 (2009)
43. A. Attwood, J. Edwards, C.C. Rowlands, D.M. Murphy, J. Phys. Chem. A **107**, 1779 (2003)
44. C.A. Jenkins, D.M. Murphy, J. Phys. Chem. B **103**, 1019 (1999)
45. D.C. Hurum, K.A. Gray, T. Rajh, M.C. Thurnauer, J. Phys. Chem. B **109**, 977 (2005)
46. S. Livraghi, M. Chiesa, M. Cristina, E. Giamello, J. Phys. Chem. C **115**, 25413 (2011)
47. S. Livraghi, M. Rolando, S. Maurelli, M. Chiesa, M. Cristina, E. Giamello, J. Phys. Chem. C **118**, 22141 (2014)
48. A.R. Gonzalez-Elipe, M. Che, J. De Chim. Phys. Phys. Chim. Biol. **79**, 355 (1982)
49. M.D. Sevilla, D. Becker, M.Y. Yan, J. Chem. Soc. Faraday Trans. **86**, 3279 (1990)

Publisher's Note Springer Nature remains neutral with regard to jurisdictional claims in published maps and institutional affiliations.